








PAPER

Effect of skin conductivity on the electric field induced by transcranial stimulation techniques in different head models

RECEIVED
16 July 2020REVISED
29 October 2020ACCEPTED FOR PUBLICATION
25 November 2020PUBLISHED
25 January 2021Micol Colella¹ , Alessandra Paffi¹ , Valerio De Santis² , Francesca Apollonio¹  and Micaela Liberti¹ ¹ Department of Information Engineering, Electronics and Telecommunications (DIET), University of Rome 'La Sapienza', Rome, Italy² Department of Industrial and Information Engineering and Economics (DIIEE), University of L'Aquila, L'Aquila, ItalyE-mail: alessandra.paffi@uniroma1.it**Keywords:** LF dosimetry, head model, skin conductivity, transcranial magnetic stimulation (TMS), transcranial direct current stimulation (tDCS)Supplementary material for this article is available [online](#)**Abstract**

This study aims at quantifying the effect that using different skin conductivity values has on the estimation of the electric (E)-field distribution induced by transcranial magnetic stimulation (TMS) and transcranial direct current stimulation (tDCS) in the brain of two anatomical models. The induced E -field was calculated with numerical simulations inside MIDA and Duke models, assigning to the skin a conductivity value estimated from a multi-layered skin model and three values taken from literature. The effect of skin conductivity variations on the local E -field induced by tDCS in the brain was up to 70%. In TMS, minor local differences, in the order of 20%, were obtained in regions of interest for the onset of possible side effects. Results suggested that an accurate model of the skin is necessary in all numerical studies that aim at precisely estimating the E -field induced during TMS and tDCS applications. This also highlights the importance of further experimental studies on human skin characterization, especially at low frequencies.

1. Introduction

Transcranial magnetic and electric stimulations are techniques that use electric or magnetic fields for the treatment of several neuronal and psychiatric disorders (Ilmoniemi *et al* 1999, Nitsche *et al* 2008). Differently from other clinical applications, such as deep brain stimulation (Okun and Zeilman 2014, Paffi *et al* 2015a), transcranial stimulation techniques have the great advantage of being non-invasive treatments.

Among them, the most widespread ones are transcranial magnetic stimulation (TMS) and transcranial direct current stimulation (tDCS). In TMS applications, an intense sinusoid-like pulsed current, varying in time at a rate of a few kHz, flows through a coil placed on the scalp. Time-varying current generates a time-varying magnetic field that, in turns, induces an electric (E)-field inside the brain. If the E -field induced in specific cortical regions overcomes a threshold level, it is thought to directly activate neuronal axons (Kammer *et al* 2011), even though other interaction mechanisms are not excluded (Bungert *et al* 2017). TMS is generally used for the treatment of schizophrenia (Rotenberg *et al* 2014, Ray *et al* 2015, Bais *et al* 2017), epilepsy (Rotenberg 2010, Vanhaerents *et al* 2020), Parkinson's disease (Chen and Chen 2019, Nardone *et al* 2020), tinnitus (Schoiswohl *et al* 2019) and depression (Valero-Cabr e *et al* 2011, Habib *et al* 2018, Kumar *et al* 2018). Other interesting possible applications are currently under investigation, including obsessive compulsive disorder (Zhou *et al* 2017, Carmi *et al* 2018), post-stroke rehabilitation (Watanabe *et al* 2018, Zhao *et al* 2018, Fiscaro *et al* 2019, He *et al* 2020), chronic pain (Yang and Chang 2020), dependencies, addiction and dementia, (Najib *et al* 2011, Horvath *et al* 2014, Lefaucheur *et al* 2014).

Conversely, tDCS makes use of a low-intensity (260 μ A–2 mA) direct current flowing between two metallic electrodes placed on the scalp (Priori *et al* 1998, Nitsche and Paulus 2001, Nitsche *et al* 2008). The induced E -field penetrates deep inside the brain but its strength is several orders of magnitude lower than in TMS so that it modulates the spontaneous neuronal activity (Nitsche and Paulus 2001, Knotkova *et al* 2019) by means of

mechanisms allowing neuronal detection of weak signals (Gammaitoni *et al* 1998, Paffi *et al* 2013). Possible clinical applications for tDCS are the treatment of psychiatric disorders, such as depression (Kekic *et al* 2016, Brunoni and Palm 2019) and, depending on the electrodes position on the scalp and polarity of stimulation, beneficial effects have been found when applying tDCS to patients affected by schizophrenia (Mondino *et al* 2015, Fröhlich *et al* 2016), neuropathic pain (David *et al* 2018), for stroke rehabilitation (Elsner *et al* 2018, Fleming *et al* 2018) and Parkinson's disease (Fregni *et al* 2006, Nitsche *et al* 2008, Lattari *et al* 2017, Dobbs *et al* 2018). For both techniques, the accurate placement of the coil or the electrodes in correspondence of the target brain region can be supported by the use of neuro-navigation systems, which grant to visualize a 3D model of the subject's brain and track the position of the coil/electrodes with respect to it (Comeau 2014, Krieg *et al* 2017, De Witte *et al* 2018). Further optimization of a TMS or a tDCS treatment derives from an accurate knowledge of the E -field distribution inside the brain. This allows to predict the stimulated brain areas, as well as to optimize both stimulation techniques during the treatment. In fact, especially in TMS applications, the most advanced neuro-navigation systems include real-time E -field calculation while placing the coil over the scalp, in order to simultaneously facilitate the best coil position and the best stimulation parameters (Hannula *et al* 2005, Ruohonen and Karhu 2010, Nummenmaa *et al* 2013, Comeau 2014, Paffi *et al* 2015b). Both real-time and offline dosimetric calculations have always played a key role to optimize TMS and tDCS applications and to understand their interaction with the neuronal tissue. Many papers were published in the last years aiming at numerically evaluating the E -field distribution induced by TMS (Deng *et al* 2013, Opitz *et al* 2014, 2016, Paffi *et al* 2015b, Bungert *et al* 2017, Laakso 2018, Gomez *et al* 2020, Weise *et al* 2020) and tDCS (Datta *et al* 2009, 2010, 2011, Truong *et al* 2013, Parazzini *et al* 2011, 2015, Manoli *et al* 2017, Fiocchi *et al* 2018, Opitz *et al* 2018, Laakso *et al* 2015, 2018a, Puonti *et al* 2019) inside the brain. These papers used different calculation methods and human head models, that spanned from simple homogeneous or multilayered spheres (Miranda *et al* 2003, 2006, De Deng *et al* 2013) up to realistic patient-specific or standard anatomical models obtained from magnetic resonance images (Starzyński *et al* 2002, Salinas *et al* 2009, Datta *et al* 2009, 2010, 2011, Chen and Mogul 2010, Parazzini *et al* 2011, 2015, Truong *et al* 2013, Paffi *et al*, 2015b, Fiocchi *et al* 2018, Laakso *et al* 2015, 2018a, 2018b, Gomez *et al* 2020). Neuro-navigation systems usually consider spherical geometries or anatomical head models that count for few tissues, given the need of a real-time E -field computation (Paffi *et al* 2015b, Krieg *et al* 2017). The offline dosimetric studies, like those used for the treatment planning, may consider patient-specific and semi-specific models (Colella *et al* 2020) as well as standard detailed anatomical head models. These models include a fine and detailed representation of different tissues and brain structures and are obtained from high-resolution MRIs scans (1 mm or less), such as those from the Virtual Population (Gosselin *et al* 2014), the Japanese models (Nagaoka *et al* 2004), MIDA (Iacono *et al* 2015), and others (Makris *et al* 2008), or are based on freely available online anatomy atlas, such as the Alvar model by Laakso and co-workers (Laakso 2018).

Although the available anatomical models are getting increasingly accurate and realistic, the assignment of dielectric properties to different tissues remains an important question. Comprehensive databases are available to furnish a reference value for permittivity and conductivity of different human tissues (Gabriel *et al* 1996, 2009, Hasgall *et al* 2018), nevertheless, there is no agreement on the value used by the different dosimetric studies currently published, especially regarding the conductivity of the skin. This wide range of values used for skin conductivity is partially due to the lack of an accurate knowledge of skin dielectric properties, especially at DC or in the low frequency (LF) range, up to 10 kHz (De Santis *et al* 2015, 2016). Furthermore, skin properties strongly depend on internal, physiologic or pathologic conditions, and on external, environmental or experimental factors (Tarao *et al* 2012). In fact, skin conductivity is highly variable with hydration level, corneum layer thickness, healthy or ill status, subject age, gender and the body part considered. Moreover, factors external to the body, such as environmental temperature and humidity or the presence of sponges and electrodes, can considerably modify skin conductivity (Tarao *et al* 2012).

The impact of skin conductivity on the estimated induced E -field was studied for safety assessment purposes under a uniform B -field, corresponding to the reference level for the general public (ICNIRP 2010) at frequencies up to 1 MHz (Schmid *et al* 2013), and it was found to be less than 15% at the level of the Central Nervous System (CNS). However, differences up to a factor of 100 were found in specific regions of the skin where pain receptors are located (Schmid *et al* 2013).

When simulating TMS applications, authors may not consider an accurate skin model and include the head's outer tissues (skin, fat, muscle) in a single layer of scalp (De Lucia *et al* 2007, Thielscher *et al* 2011, Datta *et al* 2013, Opitz *et al* 2014, Gomez *et al* 2020, Weise *et al* 2020). This choice is acceptable when assuming that the induced primary E -field, which is proportional to the time derivative of the magnetic B -field, predominates over the secondary E field, related to the charge accumulation at the interface between two tissues. Nonetheless, variability in skin thickness was shown to affect the induced electric field in the brain with changes below 5%, and up to 11% locally in the skin (Rashed *et al* 2019). A recent study on a simple multilayered sphere revealed that a 15% change in the skin conductivity, caused a variation of about 1% on the induced E -field in the brain,

however much less than those induced by other sources of variability, such as the uncertainty in coil positioning (Gomez *et al* 2015, 2018). In a preliminary study (Colella *et al* 2019) with the TMS coil placed at the top of the head of two anatomical models, the authors found that skin conductivity affected the maximum and the average E -field in the brain in a negligible way with respect to the anatomical differences. Despite the low percentage variations found in previous studies, further investigation of local differences is needed, specially where pain receptors are located, as this would be the site of possible side effects onset.

However, variability over the skin conductivity in realistic anatomical models deserves to be further investigated in different anatomical regions for an accurate estimation of the induced E -field, not only to assess TMS efficacy but also to control possible side effects, particularly on the local pain receptors on the skin (Rossini *et al* 2015). Beside the global statistical values on the E -field in single tissues, sensitive observables comparing local E -field distributions should be considered as well (Armstrong 1978).

For what concerns tDCS, the effect of outer tissue layers on the E -field induced in the brain is instead supposed to be much higher than in TMS, due to the capacitive coupling. This was also confirmed by a recent sensitivity study on a simplified anatomical model that included five different tissues (Saturnino *et al* 2019). Moreover, since the clinical response to tDCS varies from patient to patient, due to inter-individual differences in the E -field generated inside the brain (Laakso *et al* 2015, Mikkonen *et al* 2018), it is of paramount importance to quantify how much the E -field would be affected by different skin properties.

In a recent work (Huang *et al* 2017), *in vivo* intracranial recordings in epilepsy patients were used, for the first time, to validate computational head models. Validation was carried out in patient-specific models, including five different tissues, by assigning them the conductivity values that minimized the error between measurements and simulations, thus proposing a range of skin conductivity values supported indirectly by experiments.

Herein we proposed an alternative approach to estimate the skin conductivity in detailed generic anatomic head models, for which experimental validation is not feasible. It is based on numerical simulations on a multilayered skin model (De Santis *et al* 2015) and was used to estimate an average skin conductivity value suitable for the two realistic and accurate anatomical models: MIDA (Iacono *et al* 2015) and Duke (Christ *et al* 2010).

Beside this value, after an extensive literature review, we herein considered other three skin conductivities, which represented the whole range of values assigned in the literature. By means of computational simulations we rigorously quantified, with global and local sensitive observables, the influence of skin conductivity on the E -field distribution induced inside MIDA and Duke, by TMS and tDCS applicators placed on the motor cortex.

The final aim of the present work is to demonstrate the importance of an accurate skin model for a precise estimation of the simulated E -field. Moreover, we provide reliable indications on which conductivity value should be used once the level of detail considered when modeling the skin is known. This would be a solid support to all the numerical studies that want to correlate the induced E -field to the therapeutic response and/or to possible side effects.

2. Models and methods

2.1. Brief review of skin conductivity values used in literature

As reported in De Santis *et al* (2015), skin consists of several layers (stratum corneum, cellular epidermis and dermis) with different thicknesses and conductivities, thus an homogenization procedure is often considered (De Santis *et al* 2016).

In the literature dealing with LF dosimetry (from DC to 10 kHz), skin conductivity σ_s assumes several values (from 0.0002 S m^{-1} up to 0.465 S m^{-1}) spanning more than three orders of magnitude, as summarized in table 1.

The lowest value of σ_s found in literature is 0.0002 S m^{-1} , it is reported in the generic IT²IS database (Hasgall *et al* 2018) and refers to the dry skin as predicted by the dispersive model of Gabriel *et al* (1996) from 10 Hz to 10 kHz.

The highest σ_s is 0.465 S m^{-1} . It was derived in Wagner *et al* (2004) and typically refers to the scalp, a thick homogeneous tissue that incorporates the skin and the subcutaneous adipose tissue (SAT), as well as the fat and the muscle. Two noteworthy intermediate values for σ_s are 0.08 and 0.17 S m^{-1} . The latter is reported in the low-frequency IT²IS database (Hasgall *et al* 2018) and was obtained by extrapolating experimental values in accordance with the dispersion characteristics of biological tissues (Yamamoto and Yamamoto 1976).

The value 0.08 S m^{-1} is used in two models in which skin and fat are considered as a unique tissue (Laakso *et al* 2015, 2018a), and corresponds to the conductivity of the fat as reported in Gabriel *et al* (2009).

2.2. A multi-layered model for skin conductivity estimation

To restrict the range of possible σ_s to be used in numerical simulations, the level of detail chosen to model the skin should be considered. As an example, both Duke and MIDA models have an average skin thickness of

Table 1. Values of skin conductivity (σ_s) (1st column) and related reference (2nd column) used in numerical studies (3rd column) dealing with different kinds of exposure (4th column) and frequencies (5th column).

σ_s ($S m^{-1}$)	Reference for σ_s	Papers	Kind of exposure	Frequency (Hz)
0.0002	IT'IS database (Hasgall et al 2018); (Gabriel et al 1996) (dry skin)	(Tarao et al 2012, Lu and Ueno 2017, Fiocchi et al 2018)	Contact currents; short magnetic dipole; tDCS; TMS	$<10^6$
0.00045	Gabriel et al (1996) (wet skin)	Aonuma et al (2018)	TMS	10^4
0.012	Parazzini et al (2011)	Parazzini et al (2012, 2014, 2015)	tDCS	0
0.08	Gabriel et al (2009) (Same as fat)	Laakso et al (2015, 2018a)	tDCS	0
0.1	Dimbylow (1998)	Dimbylow (1998, 2005), Hirata et al (2010, 2011), Laakso and Hirata (2012), Tarao et al (2012), Laakso et al (2014)	Uniform B; contact currents; TMS	$30-10^6$
0.17	IT'IS database, low freq (Hasgall et al 2018); (Yamamoto and Yamamoto 1976)	—	—	$1-10^6$
0.20	Dawson et al (1998); Gabriel et al (2009)	Dawson et al (1998), De Santis et al (2015)	Uniform B	$1-10^4$
0.22	Hauelsen et al (1997)	Im et al (2008)	tDCS	<2
0.25	Truong et al (2013)	Bungert et al (2017)	TMS	$\leq 10^4$
0.29	Huang et al (2017)	Huang et al (2017)	tDCS	1
0.33	Salinas et al (2009)	Salinas et al (2009)	TMS	$<10^4$
0.43	Hauelsen et al (1997)	Holderfer et al (2006), Im et al (2012), Neuling et al (2012), Sadleir et al (2010, 2012), Wagner et al (2014)	tDCS,	0; 10
0.465	Wagner et al (2004)	De Lucia et al (2007), Chen and Mogul (2010), Opitz et al (2011, 2014), Thielscher et al (2011), Datta et al (2013), Windhoff et al (2013), Janssen et al (2013, 2015), Gomez et al (2020), Weise et al (2020)	TMS, tDCS	$\leq 10^4$

1.5 mm at the level of the head (see supplementary figure S9 (available online at stacks.iop.org/PMB/66/035010/mmedia)). Thus, the lowest σ_s in table 1 (0.0002 S m^{-1}), that well describes the stratum corneum (Gabriel 1997, Birgersson *et al* 2013), which is approximately $14 \mu\text{m}$ thick, should not be extended to the whole 1.5 mm thick skin. On the other hand, the highest σ_s in table 1 (0.465 S m^{-1}) is appropriate only in simplified models, where a single thick compartment (scalp) including skin, subcutaneous adipose tissue (SAT), fat, and muscles is considered.

Therefore, to estimate what skin conductivity value should be assigned to Duke-like or MIDA-like models, a 1.5 mm thick multi-layered skin model was placed inside two metallic parallel plates (see supplementary figure S10) and simulated with Sim4Life (v. 4.4, ZMT Zurich MedTech AG, Zurich, Switzerland). The following layers were considered: stratum corneum ($14 \mu\text{m}$; $\sigma = 0.0002 \text{ S m}^{-1}$), cellular epidermis ($61 \mu\text{m}$; $\sigma = 0.009 \text{ S m}^{-1}$), dermis (1 mm; $\sigma = 0.526 \text{ S m}^{-1}$), and SAT (remaining thickness; $\sigma = 0.0417 \text{ S m}^{-1}$). Thicknesses and conductivities at 1 kHz for each layer were taken from the experimental data of Tsai *et al* (2019) and Xu and Mandal (2015). Further details are given in the Supplementary material. The calculated equivalent σ_s resulted equal to 0.08 S m^{-1} . Taking into account the variations associated to each layer, as those reported in Tsai *et al* (2019), the estimated σ_s ranged from 0.07 to 0.1 S m^{-1} . Therefore, we performed a first set of numerical simulations assigning to the skin 0.08 S m^{-1} . To account for the wide range of values reported in literature three more σ_s values were considered: 0.0002, 0.17 and 0.465 S m^{-1} .

The same values were used for both stimulation techniques, as σ_s increases by less than 2% from 10 Hz to 10 kHz (Gabriel *et al* 1996).

2.3. Head models

The anatomical models used in this work are Duke, a 34 year old male whole body model, belonging to the Virtual Population (Christ *et al* 2010), and MIDA, a 29 year old female model of head and neck (Iacono *et al* 2015).

From the whole Duke model, we extracted only the head and the neck, down to the carotid sinus, thus counting 38 different tissues, including all the basic head structures, such as the cerebrospinal fluid (CSF), gray matter (GM) and white matter (WM).

The MIDA model includes 115 separate structures, with a detailed representation of nerves and vessels.

However, to compare results obtained with the two models, we considered the same level of anatomical detail for MIDA and Duke by reducing the MIDA model to 38 different anatomical structures. This was done by merging together all tissues characterized by the same dielectric properties. By doing so, the dielectric discontinuities of the model are not altered.

Both surface-based head models were imported in the commercial software Sim4Life (Sim4Life-v4.4. SIMulation 4 LIFE Science Platform) and discretized with a maximum spatial step of 1 mm in the three orthogonal directions. Dielectric properties of all the tissues (except the skin) were taken from the IT'IS database (Gabriel *et al* 1996, Hasgall *et al* 2018) at 3 kHz for TMS and 10 Hz for tDCS. The latter is the lowest frequency at which measurements have been conducted (Gabriel *et al* 1996).

2.4. tDCS electrodes model

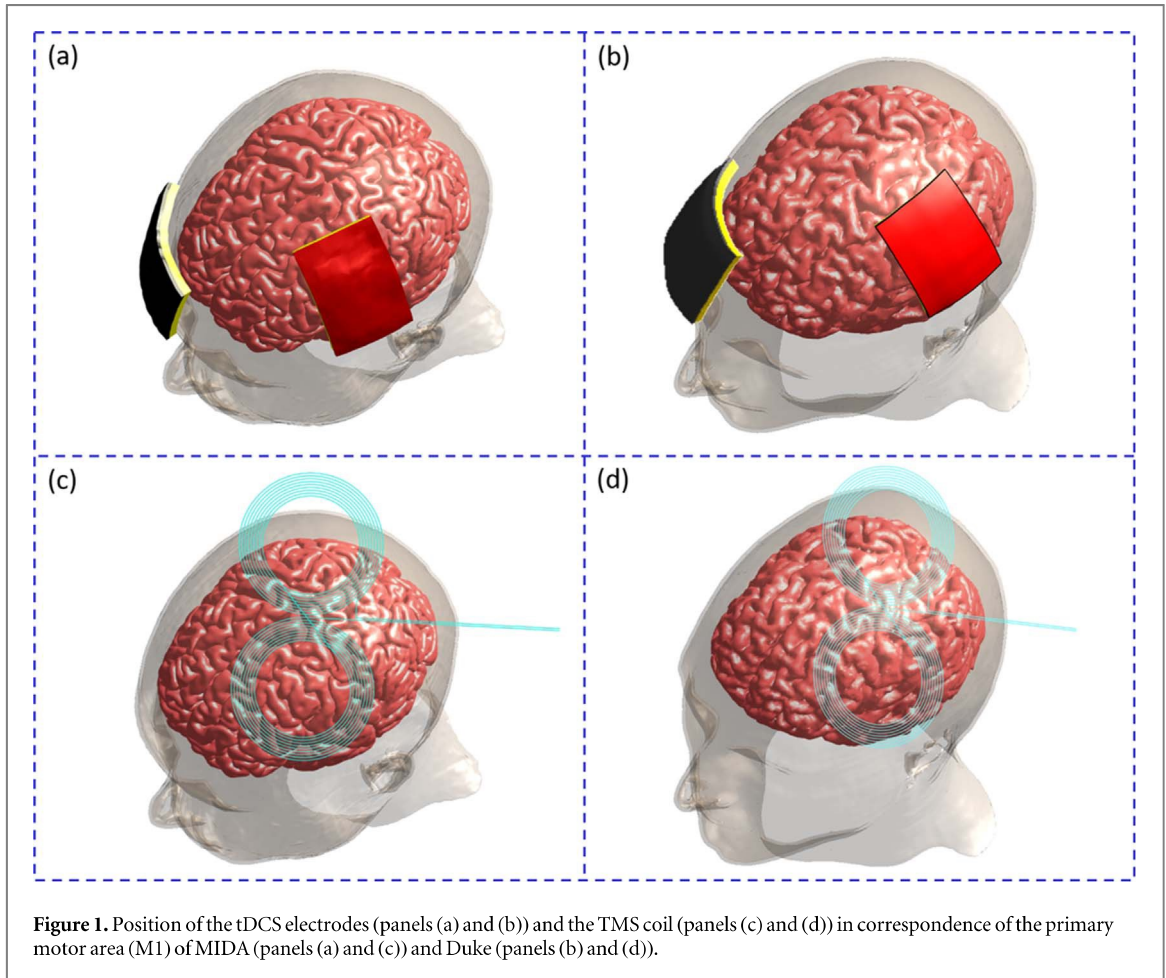
tDCS electrodes were modeled as two rectangular pads of $5 \text{ cm} \times 7 \text{ cm}$ that consisted of a metallic contact, modeled as Perfect Electric Conductor (PEC), and a saline soaked sponge ($\sigma = 1.4 \text{ S m}^{-1}$) between the electrode and the scalp (see figures 1(a) and (b)). The cathode, colored in black in figure 1, was placed over the contralateral supraorbital region, while the anode, colored in red, was placed over the primary motor cortex (M1) (Nitsche *et al* 2008). M1 is anterior to the central sulcus and is one the most commonly targeted areas in both tDCS and TMS (Opitz *et al* 2011, Thielscher *et al* 2011, Laakso *et al* 2014). The different positioning of the anode between MIDA and Duke, see figures 1(a) and (b), is due to the anatomical differences in the cortical circulations, specifically in the central sulcus.

The electromagnetic (EM) problem was solved with the EM simulation software Sim4Life using the electro ohmic quasi-static solver, which solves the Laplace equation. Simulations were performed injecting a current of 1 mA into the head.

2.5. TMS coil model

The two head models were exposed to a commercial figure-of-eight coil (PN9925-00, MagStim Eden Prairie, MN), modeled as a current pathway made of two coplanar windings, 9 turns each, with the internal diameter of 6 cm and the external diameter of 8.6 cm, as described in Paffi *et al* (2015b) (figures 1(c) and (d)). The coil was placed at a distance of 5 mm from the scalp in correspondence of M1 (Janssen *et al* 2015).

According to the specifications of the neurostimulator ('MAGSTIM[®] RAPID2, P/N 3576-23-09, OPERATING MANUAL'), the frequency was set to 3 kHz and the current amplitude was such to obtain a *B*-field



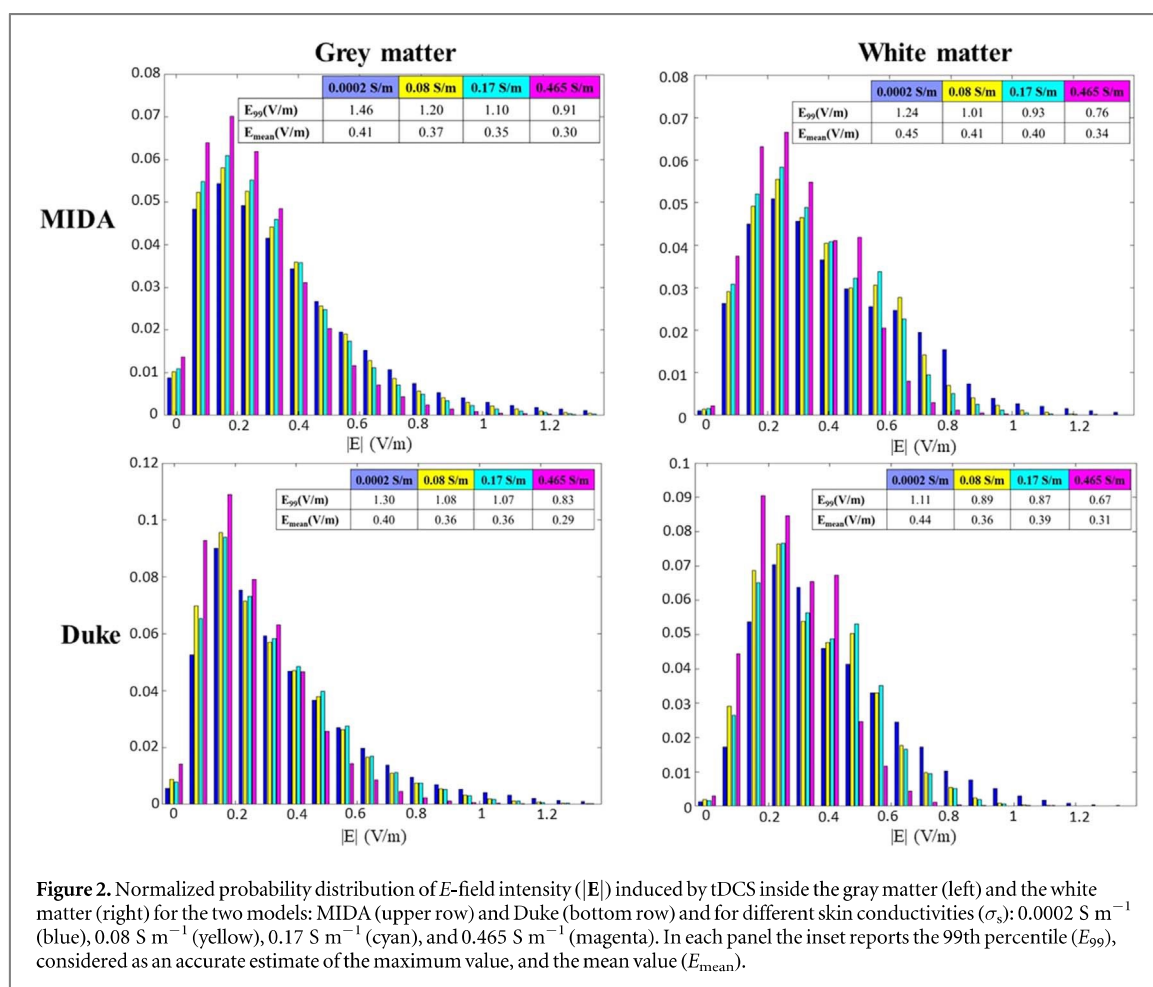
of 1.2 T on the scalp surface just below the coil. The problem was solved using the Magneto Quasi-Static (MQS) module included in the LF solver of the EM simulation software Sim4Life.

2.6. Observables

For each different tissue, the E -field distribution was considered. Starting from that, the mean value, the maximum value and the percentiles were extracted to compare results obtained with different head models and σ_s . To avoid numerical artifacts, the 99th percentile was used as an estimation of the maximum value of the E -field (E_{\max}), as suggested by the ICNIRP guidelines of 2010, (ICNIRP 2010). To estimate E_{\max} , other papers proposed either to use a dynamic approach (De Santis and Chen 2014) or to use the 99.9th and even the 99.99th percentile (Soldati and Laakso 2020). However, looking at the probability distributions of the E -field intensity inside the WM and the GM in our simulations, we decided to follow the ICNIRP guidelines and to use the 99th percentile (see supplementary material and figures S1–S8). Beside this global evaluation, to compare voxel-by-voxel the E -field distribution obtained with different σ_s , and to quantify differences in regions that are distant from the stimulation focus, we calculated the symmetric mean absolute percentage error (SMAPE) (Armstrong 1978) defined as:

$$\text{SMAPE}(i, j, k) = \frac{|E_{\sigma}(i, j, k) - E_{\sigma_{\text{REF}}}(i, j, k)|}{\left(\frac{E_{\sigma}(i, j, k) + E_{\sigma_{\text{REF}}}(i, j, k)}{2}\right)} \times 100,$$

where i, j and k are the indexes of the single voxel, while $E_{\sigma}(i, j, k)$ and $E_{\sigma_{\text{REF}}}(i, j, k)$ are the intensity of the E -field for the evaluated conductivity (σ) and the reference conductivity (σ_{REF}) computed in the voxel (i, j, k) . For the sake of convenience, we used as the reference skin conductivity (σ_{REF}) the lowest one: 0.0002 S m^{-1} .



3. Results

3.1. tDCS

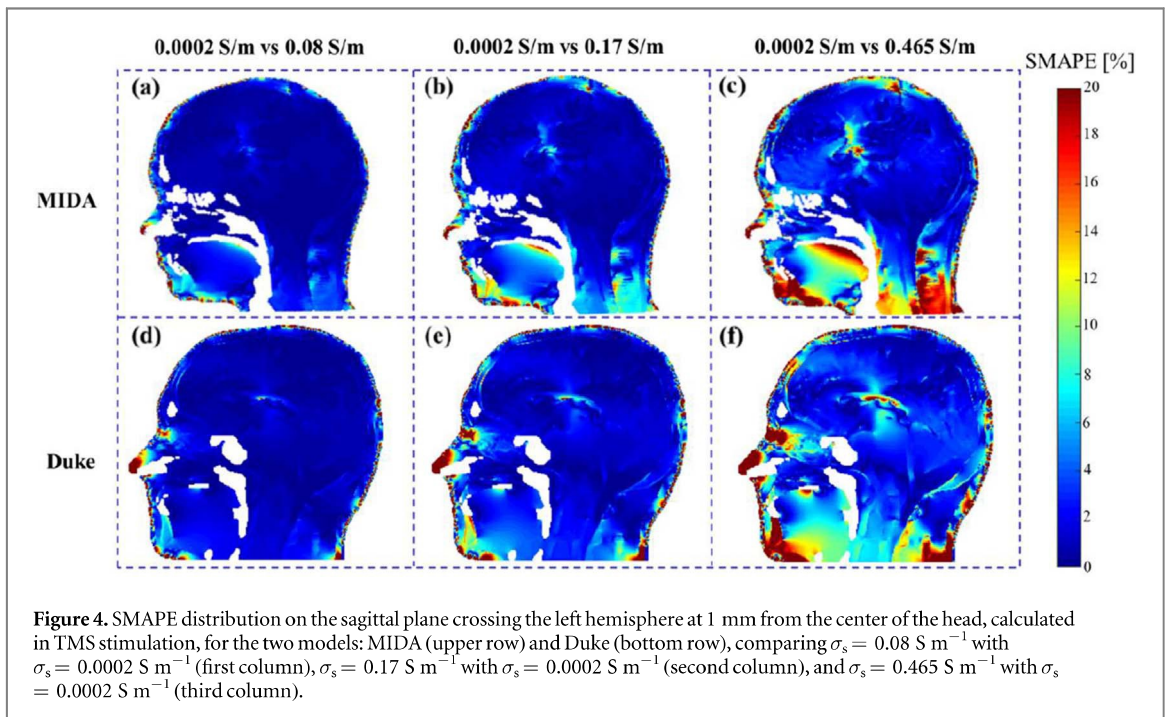
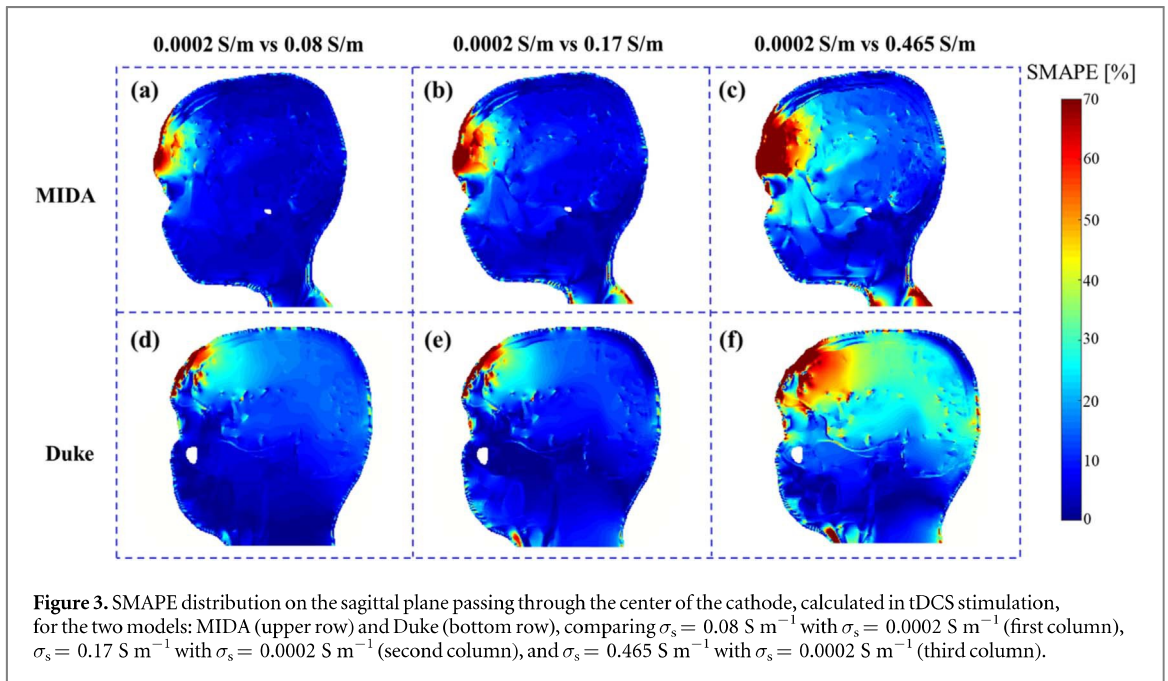
Probability distributions of the calculated E -field intensity inside the tissues involved in the stimulation, i.e. GM and WM, for MIDA and Duke are shown in figure 2, together with the average value (E_{mean}) and the 99th percentile (E_{99}), reported in the inset of each panel.

Comparing the different anatomical models, for both tissues, one can see that the distributions are very similar, with a maximum value around 1 V m⁻¹ for almost all the investigated conductivities, as expected from literature (Parazzini *et al* 2011, Truong *et al* 2013). Higher values are induced in MIDA, probably due to the smaller size of the head (23 cm × 21.6 cm × 16.3 vs 23.4 cm × 24 cm × 18 cm), with maximum differences between the models equal to about 12% for both E_{99} and E_{mean} . This result was in line with those obtained in Parazzini *et al* (2014), where both peak and median values of the E -field amplitude were higher in a child model than in adult ones. Both in Duke and MIDA, an increase of σ_s led to a reduction of the induced E -field in the inner structures due to a higher voltage drop across the skin layer. Maximum variations on E_{99} and E_{mean} were, respectively, about 40% and 25% for MIDA model and 40% and 30% for Duke. This implied that the choice of skin conductivity might affect the predicted induced E -field in the brain even more than the considered anatomical model.

Moving to the local differences, figure 3 shows the SMAPE on a sagittal plane passing through the center of the cathode for MIDA (upper row) and Duke (bottom row), calculated between each conductivity value and the 'reference' value of 0.0002 S m⁻¹. Maximum differences were in the frontal region below the anode, and might reach values as high as 70% even inside the brain, revealing that prediction of stimulated areas strongly depends on the correct choice of skin conductivity.

3.2. TMS

The same analysis on statistical values conducted for TMS application revealed that the induced E -field in the brain (GM and WM) was less sensitive to both the anatomical model and the skin conductivity than it was in tDCS (data reported in supplementary tables S1 and S2).



Variability between MIDA and Duke reached 11% for E_{99} and 1.5% for E_{mean} inside GM, whereas, for both models, the effect of skin conductivity on E_{99} and E_{mean} in the brain (GM and WM) was negligible, less than 1% (data reported in the Supplementary material). This was expected given that the induced E -field follows closed streamlines, as the eddy currents. Therefore, just below the coil, it is almost tangential to the air-skin and skin-SAT boundaries and is only slightly affected by the conductivity contrast at the interfaces (Chen *et al* 2013, De Santis *et al* 2015, 2016).

However, looking at the SMAPE on the sagittal plane of the left hemisphere at 1 mm from the center of the head, shown in figure 4, we could see that there were some regions in both models where the SMAPE was quite large. Particularly, it was higher than 10% in a region deep inside the brain, when comparing the two extreme values used for σ_s (see figures 4(c) and (f)). Similar findings were obtained in Colella *et al* (2019) with the coil placed on the top of the head. Such SMAPE distributions could be explained by the fact the effect of skin conductivity variations is more relevant on the normal component of the E -field than it is on the tangential one, and in the deep brain regions the induced E -field is mainly oriented orthogonally to the interfaces between GM, WM and CSF. The region where the SMAPE resulted to be higher than 10% was calculated to be of about 26.1 cm^3 in the MIDA model and 8.5 cm^3 in the Duke model and included areas of the WM and GM, such as

Caudate Nucleus, Accumbens Nucleus and Thalamus. Although these regions are not the preferred TMS targets, they are involved in cognitive and motor tasks and their malfunctioning is related to pathologies such as Parkinson's disease and Huntington's Core (Weber and Eisen 2002, Cincotta and Ziemann 2008, Lefaucheur *et al* 2014), attention deficit/hyperactivity disorder (Croarkin *et al* 2011, Rotenberg *et al* 2014) and obsessive-compulsive disorder (Carmi *et al* 2018). Therefore, an accurate prediction of the E -field induced in these regions could be of importance for improving the efficacy of new TMS applications while reducing side effects.

Significant SMAPE values, up to 20%, were also found in the skin and in correspondence of the carotid sinus in the neck (19.43% in the MIDA model) (see figure 4).

4. Discussion

For both head models, changes of σ_s determined variations on E_{99} and E_{mean} , induced in the brain by tDCS, up to 40% and 30%, respectively, higher than those caused by the use of different anatomical models (12%). Local percentage variations, quantified by the SMAPE, which is a sensitive local observable, reached 70% in the frontal region beneath the cathode, when comparing the highest and lowest values assigned to σ_s (0.0002 S m^{-1} and 0.465 S m^{-1}). The E -field induced inside the brain was overestimated for σ_s lower than the calculated equivalent σ_s and vice versa.

These high differences were attributed to the capacitive coupling between the source (tDCS electrodes) and the tissues, so that an impedance variation of the outermost layer (skin) likely affected also the underlying layers (GM and WM). In fact, right below the electrodes, the E -field was almost orthogonal to the tissues interfaces and thus it was strongly sensitive to impedance discontinuity.

Conversely, for TMS, the effect of skin conductivity on the induced E_{mean} and E_{99} in the brain was negligible, much lower than the variability due to the different head models on the E_{99} in GM (11%). This is expected since the induced E -field is dominated by the time derivative of B -field which is almost tangential to the interface between skin and subcutaneous tissues below the coil (Chen *et al* 2013, De Santis *et al* 2015). However, using the SMAPE, significant differences (higher than 10%) were found in the deep regions of the brain belonging to the basal ganglia. Due to the importance of such regions in cognitive, motor and sensorial functions, an accurate evaluation of the induced E -field is desirable for assessment of TMS effects. Other regions where the SMAPE assumed high values (up to 20%) were the skin and blood vessels, in correspondence of the carotid sinus. Accounting for these differences may be relevant to control the onset of side effects, such as pain sensation due to stimulation of peripheral nerves in the epidermis. Such higher differences were related to the presence of the secondary E -field, proportional to $-\nabla V$ (being V the electric scalar potential) generated by the charge accumulation at the tissue interfaces, which cannot be neglected.

This different behavior between TMS and tDCS was in line with results in Saturnino *et al* (2019), where the skin, together with other sub-cutaneous tissues, was included in a single layer (scalp) whose conductivity assumed a beta distribution between 0.2 and 0.5 S m^{-1} .

Our results, compared to those reported in the literature, suggested that the choice of skin conductivity to be used in dosimetric studies is subject to the degree of anatomical accuracy used for the skin representation in each head model.

Specifically, when considering models in which the skin is incorporated in a thick homogeneous scalp tissue, the average conductivity value that should be assigned to it would take into account all the included cutaneous and extra-cutaneous tissues (e.g. dermis, SAT, muscle).

For MIDA and Duke we suggest to use a value equal to 0.08 S m^{-1} as in (Laakso *et al* 2018a) and confirmed by our slab modeling. This value can be applied to all the models that represent the skin as a separate tissue about 1.5 mm thick. It is lower with respect to the one estimated in Huang *et al* (2017) by means of intracranial measurements (0.29 S m^{-1}). This discrepancy is attributable to the different thickness associated to the skin layer in the used models. In MIDA and Duke the skin was about 1.5 mm thick and included only a thin layer of SAT as sub-cutaneous tissue, whereas the patient-specific models used in Huang *et al* (2017) considered the skin as a thick layer of scalp, that included the muscle, which is characterized by a higher conductivity value.

5. Conclusions

The accurate estimation of the E -field induced in the brain by transcranial stimulation techniques has assumed increasing importance in the optimization of these clinical applications. Therefore, realistic dosimetric models are needed. An open question is the attribution of appropriate skin conductivity values, due to their variability with internal and external environmental factors and to the scarcity of experimental data, especially at DC.

Results of our study on two different anatomical models, MIDA and Duke, showed that variability of skin conductivity in the range reported in literature determined non-negligible differences in the E -field induced in

the brain by tDCS (globally up to 40% and locally up to 70%), much higher than those attributable to anatomical differences between the two models (12%).

Conversely, the maximum and mean E-field induced inside the brain by TMS were sensitive to the anatomical differences between the two models (11%) and almost insensitive (<1%) to changes in σ_s , as expected. Nevertheless, SMAPE values up to 20% were found on the skin, in deep brain areas and at the level of the peripheral nerves.

In summary, the choice of a representative σ_s value is fundamental to accurately predict the induced E-field correlated to the effects of tDCS observed experimentally.

Even in the TMS technique, a realistic skin model, separated from other extracutaneous tissues, should be considered to accurately simulate the induced E-field. In case it is not possible to obtain a realistic skin model, the error induced by the modeling approximation should be taken into account when estimating the E-field value induced to achieve the stimulation of target areas or that induced in non-target area.

For both techniques, the most representative skin conductivity value should be evaluated in each head model, considering the geometric and dielectric properties of the different layers that compose the skin. Therefore, this equivalent value will depend on the level of detail with which the skin of the considered head model is segmented. For MIDA and Duke models, it was estimated to be 0.08 S m^{-1} , calculated on the basis of experimental data (Tsai et al 2019) obtained from the forearm skin of healthy subjects at 1 kHz.

Further experimental studies are advisable to measure thicknesses and conductivities of the layers composing the human skin in correspondence of the head, especially at frequencies below 1 kHz. This would give a more accurate value to the skin conductivity and to its variability to be used in dosimetric studies that assess transcranial stimulation techniques.

Acknowledgments

Micaela Liberti acknowledges financial support from the Sapienza University of Rome, Research Projects, 2017 (No. RM11715C7DCB8473). Francesca Apollonio acknowledges financial support from the Sapienza University of Rome, Research Projects, 2018 (No. RM118164282B735A) and the COST Action CA15211—Atmospheric Electricity Network: coupling with the Earth System, climate and biological systems (Electronet). Authors would like to thank Matteo Luraschi and Antonio Volpe, University of L'Aquila, for their valuable support with the EM simulations and with the CAD modeling.

ORCID iDs

Micol Colella  <https://orcid.org/0000-0003-1715-9619>

Alessandra Paffi  <https://orcid.org/0000-0003-0408-8348>

Valerio De Santis  <https://orcid.org/0000-0001-6223-744X>

Francesca Apollonio  <https://orcid.org/0000-0001-6937-9731>

Micaela Liberti  <https://orcid.org/0000-0002-7494-2696>

References

- Aonuma S, Gomez-Tames J, Laakso I, Hirata A, Takakura T, Tamura M and Muragaki Y 2018 A high-resolution computational localization method for transcranial magnetic stimulation mapping *Neuroimage* **172** 85–93
- Armstrong SJ 1978 *Long-range Forecasting: From Crystal Ball to Computer* 2nd edn (Canada: Wiley-Interscience)
- Bais L, Liemburg E, Vercammen A, Bruggeman R, Knegtering H and Aleman A 2017 Effects of low frequency rTMS treatment on brain networks for inner speech in patients with schizophrenia and auditory verbal hallucinations *Prog. Neuro-Psychopharmacol. Biol. Psychiatry* **78** 105–13
- Birgersson U, Birgersson E, Nicander I and Ollmar S 2013 A methodology for extracting the electrical properties of human skin *Physiol. Meas.* **34** 723–36
- Brunoni A R and Palm U 2019 Transcranial direct current stimulation in psychiatry: mood disorders, schizophrenia and other psychiatric diseases BT *Practical Guide to Transcranial Direct Current Stimulation: Principles, Procedures and Applications* ed H Knotkova et al (Cham: Springer International Publishing) pp 431–71
- Bungert A, Antunes A, Espenhahn S and Thielscher A 2017 Where does TMS stimulate the motor cortex? Combining electrophysiological measurements and realistic field estimates to reveal the affected cortex position *Cereb. Cortex* **27** 5083–94
- Carmi L, Alyagon U, Barnea-Ygaël N, Zohar J, Dar R and Zangen A 2018 Clinical and electrophysiological outcomes of deep TMS over the medial prefrontal and anterior cingulate cortices in OCD patients *Brain Stimul.* **11** 158–65
- Chen K H S and Chen R 2019 Invasive and noninvasive brain stimulation in Parkinson's disease: clinical effects and future perspectives *Clin. Pharmacol. Ther.* **106** 763–75
- Chen M and Mogul D J 2010 Using increased structural detail of the cortex to improve the accuracy of modeling the effects of transcranial magnetic stimulation on neocortical activation *IEEE Trans. Biomed. Eng.* **57** 1216–26
- Chen X L, Benkler S, Chavannes N, De Santis V, Bakker J, van Rhoon G, Mosig J and Kuster N 2013 Analysis of human brain exposure to low-frequency magnetic fields: a numerical assessment of spatially averaged electric fields and exposure limits *Bioelectromagnetics* **34** 375–84

- Christ A et al 2010 The virtual family—development of surface-based anatomical models of two adults and two children for dosimetric simulations *Phys. Med. Biol.* **55** N23
- Cincotta M and Ziemann U 2008 Neurophysiology of unimanual motor control and mirror movements *Clin. Neurophysiol.* **119** 744–62
- Colella M, Camera F, Capone F, Setti S, Cadossi R, Di Lazzaro V, Apollonio F and Liberti M 2020 Patient semi-specific computational modeling of electromagnetic stimulation applied to neuroprotective treatments in acute ischemic stroke *Sci. Rep.* **10** 1–12
- Colella M, Paffi A, Fontana S, Rossano F, De Santis V, Apollonio F and Liberti M 2019 Influence of anatomical model and skin conductivity on the electric field induced in the head by transcranial magnetic stimulation *Proc. Annu. Int. Conf. IEEE Eng. Med. Biol. Soc. EMBS* pp 2917–20
- Comeau R 2014 Neuronavigation for transcranial magnetic stimulation *Transcranial Magnetic Stimulation* ed A Rotenberg, J C Horvath and A Pascual-Leone (New York: Springer) pp 31–56
- Croarkin P E, Wall C A and Lee J 2011 Applications of transcranial magnetic stimulation (TMS) in child and adolescent psychiatry *Int. Rev. Psychiatry* **23** 445–53
- Datta A, Baker J M, Bikson M and Fridriksson J 2011 Individualized model predicts brain current flow during transcranial direct-current stimulation treatment in responsive stroke patient *Brain Stimul.* **4** 169–74
- Datta A, Bansal V, Diaz J, Patel J, Reato D and Bikson M 2009 Gyri-precise head model of transcranial direct current stimulation: improved spatial focality using a ring electrode versus conventional rectangular pad *Brain Stimul.* **2** 201–7
- Datta A, Bikson M and Fregni F 2010 Transcranial direct current stimulation in patients with skull defects and skull plates: high-resolution computational FEM study of factors altering cortical current flow *Neuroimage* **52** 1268–78
- Datta A, Zhou X, Su Y, Parra L C and Bikson M 2013 Validation of finite element model of transcranial electrical stimulation using scalp potentials: Implications for clinical dose *J. Neural Eng.* **10** N3
- David M C M M, de Moraes A A, de Costa M L and Franco C I F 2018 Transcranial direct current stimulation in the modulation of neuropathic pain: a systematic review *Neurol. Res.* **40** 557–65
- Dawson T W, Caputa K and Stuchly M A 1998 High-resolution organ dosimetry for human exposure to low-frequency electric fields *IEEE Trans. Power Deliv.* **13** 366–73
- De Lucia M, Parker G J M, Embleton K, Newton J M and Walsh V 2007 Diffusion tensor MRI-based estimation of the influence of brain tissue anisotropy on the effects of transcranial magnetic stimulation *Neuroimage* **36** 1159–70
- De Santis V and Chen X L 2014 On the issues related to compliance assessment of IECNIRP 2010 basic restrictions *J. Radiol. Prot.* **34** N31
- De Santis V, Chen X L, Cruciani S, Campi T and Feliziani M 2016 A novel homogenization procedure to model the skin layers in LF numerical dosimetry *Phys. Med. Biol.* **61** 4402–11
- De Santis V, Chen X L, Laakso I and Hirata A 2015 An equivalent skin conductivity model for low-frequency magnetic field dosimetry *Biomed. Phys. Eng. Express* **10** 15201
- De Witte S, Klooster D, Dedoncker J, Duprat R, Remue J and Baeken C 2018 Left prefrontal neuronavigated electrode localization in tDCS: 10–20 EEG system versus MRI-guided neuronavigation *Psychiatry Res.-Neuroimaging* **274** 1–6
- Deng Z-D, Lisanby S H and Peterchev A V 2013 Electric field depth-focality tradeoff in transcranial magnetic stimulation: simulation comparison of 50 coil designs *Brain Stimul.* **6** 1–13
- Dimbylow P 2005 Development of the female voxel phantom, NAOMI, and its application to calculations of induced current densities and electric fields from applied low frequency magnetic and electric fields *Phys. Med. Biol.* **50** 1047–70
- Dimbylow P J 1998 Induced current densities from low-frequency magnetic fields in a 2 mm resolution, anatomically realistic model of the body *Phys. Med. Biol.* **43** 221–30
- Dobbs B, Pawlak N, Biagioni M, Agarwal S, Shaw M, Pilloni G, Bikson M, Datta A and Charvet L 2018 Generalizing remotely supervised transcranial direct current stimulation (tDCS): feasibility and benefit in Parkinson's disease *J. Neuroeng. Rehabil.* **15** 1–8
- Elsner B, Bugler J and Mehrholz J 2018 Transcranial direct current stimulation (tDCS) for upper limb rehabilitation after stroke: future directions. 11 Medical and Health Sciences 1109 Neurosciences Alan Godfrey, Rodrigo Vitorio *J. Neuroeng. Rehabil.* **15** 106
- Fiocchi S, Chiaramello E, Ravazzani P and Parazzini M 2018 Modelling of the current density distributions during cortical electric stimulation for neuropathic pain treatment *Comput. Math. Methods Med.* **2018** 1–12
- Fisicaro F, Lanza G, Grasso A A, Pennisi G, Bella R, Paulus W and Pennisi M 2019 Repetitive transcranial magnetic stimulation in stroke rehabilitation: review of the current evidence and pitfalls *Ther. Adv. Neurol. Disord.* **12** 1–22
- Fleming M K, Theologis T, Buckingham R and Johansen-Berg H 2018 Transcranial direct current stimulation for promoting motor function in cerebral palsy: a review *J. Neuroeng. Rehabil.* **15** 1–8
- Fregni F, Boggio P S, Santos M C, Lima M, Vieira A L, Rigonatti S P, Silva M T A, Barbosa E R, Nitsche M A and Pascual-Leone A 2006 Noninvasive cortical stimulation with transcranial direct current stimulation in Parkinson's disease *Mov. Disord.* **21** 1693–702
- Fröhlich F, Burrello T N, Mellin J M, Cordle A L, Lustenberger C M, Gilmore J H and Jarskog L F 2016 Exploratory study of once-daily transcranial direct current stimulation (tDCS) as a treatment for auditory hallucinations in schizophrenia *Eur. Psychiatry* **33** 54–60
- Gabriel C 1997 Comments on 'dielectric properties of the skin' *Phys. Med. Biol.* **42** 1671–3
- Gabriel C, Peyman A and Grant E H 2009 Electrical conductivity of tissue at frequencies below 1 MHz *Phys. Med. Biol.* **54** 4863
- Gabriel S, Lau R W and Gabriel C 1996 The dielectric properties of biological tissues: II. Measurements in the frequency range 10 Hz–20 GHz *Phys. Med. Biol.* **41** 2251–69
- Gammaitoni L, Hanggi P, Jung P and Marchesoni F 1998 Stochastic resonance *Rev. Mod. Phys.* **70** 223–87
- Gomez L J, Dannhauer M, Koponen L M and Peterchev A V 2020 Conditions for numerically accurate TMS electric field simulation *Brain Stimul.* **13** 157–66
- Gomez L J, Goetz S M and Peterchev A V 2018 Design of transcranial magnetic stimulation coils with optimal trade-off between depth, focality, and energy *J. Neural Eng.* **15** 1–31
- Gomez L J, Yücel A C, Hernandez-Garcia L, Taylor S F and Michielssen E 2015 Uncertainty quantification in transcranial magnetic stimulation via high-dimensional model representation *IEEE Trans. Biomed. Eng.* **62** 361–72
- Gosselin M-C et al 2014 Development of a new generation of high-resolution anatomical models for medical device evaluation: the virtual population 3.0 *Phys. Med. Biol.* **59** 5287–303
- Habib S, Hamid U, Jamil A, Zainab A Z, Yousuf T, Habib S, Tariq S M and Ali F 2018 Transcranial magnetic stimulation as a therapeutic option for neurologic and psychiatric illnesses *Cureus* **10** e3456
- Hannula H, Ylioja S, Pertovaara A, Korvenoja A, Ruohonen J, Ilmoniemi R J and Carlson S 2005 Somatotopic blocking of sensation with navigated transcranial magnetic stimulation of the primary somatosensory cortex *Hum. Brain Mapp.* **26** 100–9
- Hasgall P, Di Gennaro F, Baumgartner C, Neufeld E, Lloyd B, Gosselin M, Payne D, Klingensböck A and Kuster N 2018 Tissue Properties Database V4.0

- Hausein J, Ramon C, Eiselt M, Brauer H and Nowak H 1997 Influence of tissue resistivities on neuromagnetic fields and electric potentials studied with a finite element model of the head *IEEE Trans. Biomed. Eng.* **44** 727–35
- He Y, Li K, Chen Q, Yin J and Bai D 2020 Repetitive transcranial magnetic stimulation on motor recovery for patients with stroke: a PRISMA compliant systematic review and meta-analysis *Am. J. Phys. Med. Rehabil.* **99** 99–108
- Hirata A, Takano Y, Fujiwara O, Dovan T and Kavet R 2011 An electric field induced in the retina and brain at threshold magnetic flux density causing magnetophosphenes *Phys. Med. Biol.* **56** 4091–101
- Hirata A, Takano Y, Kamimura Y and Fujiwara O 2010 Effect of the averaging volume and algorithm on the *in situ* electric field for uniform electric- and magnetic-field exposures *Phys. Med. Biol.* **55** N243
- Holdefer R N, Sadleir R and Russell M J 2006 Predicted current densities in the brain during transcranial electrical stimulation *Clin. Neurophysiol.* **117** 1388–97
- Horvath J C, Najib U and Press D Z 2014 Transcranial magnetic stimulation (TMS) clinical applications: therapeutics *Transcranial Magnetic Stimulation* ed A Rotenberg, J Horvath and A Pascual-Leone (New York: Springer) pp 235–57
- Huang Y, Liu A A, Lafon B, Friedman D, Dayan M, Wang X, Bikson M, Doyle W K, Devinsky O and Parra L C 2017 Measurements and models of electric fields in the *in vivo* human brain during transcranial electric stimulation *Elife* **6** 1–26
- Iacono M I et al 2015 MIDA: a multimodal imaging-based detailed anatomical model of the human head and neck *PLoS One* **10** e0124126
- International Commission on Non-Ionizing Radiation Protection 2010 Guidelines for limiting exposure to time-varying electric and magnetic fields (1 Hz–100 kHz) *Health Phys.* **99** 818–36
- Ilmoniemi R, Ruohonen J and Karhu J 1999 Transcranial magnetic stimulation—a new tool for functional imaging of the brain *Crit. Rev. Biomed. Eng.* **27** 241–84
- Im C H, Jung H H, Choi J D, Lee S Y and Jung K Y 2008 Determination of optimal electrode positions for transcranial direct current stimulation (tDCS) *Phys. Med. Biol.* **53** N219
- Im C H, Park J H, Shim M, Chang W H and Kim Y H 2012 Evaluation of local electric fields generated by transcranial direct current stimulation with an extracerebral reference electrode based on realistic 3D body modeling *Phys. Med. Biol.* **57** 2137–50
- Janssen A M, Oostendorp T F and Stegeman D F 2015 The coil orientation dependency of the electric field induced by TMS for M1 and other brain areas *J. NeuroEng. Rehabil.* **12** 1–13
- Janssen A M, Rampersad S M, Lucka F, Lanfer B, Lew S, Aydin Ü, Wolters C H, Stegeman D F and Oostendorp T F 2013 The influence of sulcus width on simulated electric fields induced by transcranial magnetic stimulation *Phys. Med. Biol.* **58** 4881–96
- Kammer T, Beck S, Thielscher A, Laubis-Herrmann U and Topka H 2011 Motor thresholds in humans: a transcranial magnetic stimulation study comparing different pulse waveforms, current directions and stimulator types *Clin. Neurophysiol.* **112** 250–8
- Kekic M, Boysen E, Campbell I C and Schmidt U 2016 A systematic review of the clinical efficacy of transcranial direct current stimulation (tDCS) in psychiatric disorders *J. Psychiatr. Res.* **74** 70–86
- Knotkova H, Nitsche M A, Bikson M and Woods A J 2019 *Practical Guide to Transcranial Direct Current Stimulation: Principles, Procedures and Applications* (Cham: Springer) (https://doi.org/10.1007/978-3-319-95948-1_1)
- Krieg S M et al 2017 Protocol for motor and language mapping by navigated TMS in patients and healthy volunteers; workshop report *Acta Neurochir.* **159** 1187–95
- Kumar S, Singh S, Parmar A, Verma R and Kumar N 2018 Effect of high-frequency repetitive transcranial magnetic stimulation (rTMS) in patients with comorbid panic disorder and major depression *Australas. Psychiatry* **26** 398–400
- Laakso I 2018 Alvar: Adult whole-body anatomic phantom for computational dosimetry, Project website <https://version.aalto.fi/gitlab/ilaakso/alvar/>
- Laakso I and Hirata A 2012 Reducing the staircasing error in computational dosimetry of low-frequency electromagnetic fields *Phys. Med. Biol.* **57** N25
- Laakso I, Hirata A and Ugawa Y 2014 Effects of coil orientation on the electric field induced by TMS over the hand motor area *Phys. Med. Biol.* **59** 203–18
- Laakso I, Mikkonen M, Koyama S, Ito D, Yamaguchi T, Hirata A and Tanaka S 2018a Electric field dependent effects of motor cortical tDCS [bioRxiv 327361](https://doi.org/10.1101/327361)
- Laakso I, Murakami T, Hirata A and Ugawa Y 2018b Where and what TMS activates: experiments and modeling *Brain Stimul.* **11** 166–74
- Laakso I, Tanaka S, Koyama S, De Santis V and Hirata A 2015 Inter-subject variability in electric fields of motor cortical tDCS *Brain Stimul.* **8** 906–13
- Lattari E, Costa S S, Campos C, de Oliveira A J, Machado S and Maranhao Neto G A 2017 Can transcranial direct current stimulation on the dorsolateral prefrontal cortex improve balance and functional mobility in Parkinson's disease? *Neurosci. Lett.* **636** 165–9
- Lefaucheur J-P et al 2014 Evidence-based guidelines on the therapeutic use of repetitive transcranial magnetic stimulation (rTMS) *Clin. Neurophysiol.* **125** 2150–206
- Lu M and Ueno S 2017 Comparison of the induced fields using different coil configurations during deep transcranial magnetic stimulation *PLoS One* **12** e0178422
- The MAGSTIM Company LTD 2009 MAGSTIM RAPID2 P/N 3576-23-09, OPERATING MANUAL
- Makris N, Angelone L, Tulloch S, Sorg S, Kaiser J, Kennedy D and Bonmassar G 2008 MRI-based anatomical model of the human head for specific absorption rate mapping *Med. Biol. Eng. Comput.* **46** 1239–51
- Manoli Z, Parazzini M, Ravazzani P and Samaras T 2017 The electric field distributions in anatomical head models during transcranial direct current stimulation for post-stroke rehabilitation *Med. Phys.* **44** 262–71
- Mikkonen M, Laakso I, Sumiya M, Koyama S, Hirata A and Tanaka S 2018 TMS motor thresholds correlate with tDCS electric field strengths in hand motor area *Front. Neurosci.* **12** 426
- Miranda P C, Hallett M and Basser P J 2003 The electric field induced in the brain by magnetic stimulation: a 3-D finite-element analysis of the effect of tissue heterogeneity and anisotropy *IEEE Trans. Biomed. Eng.* **50** 1074–85
- Miranda P C, Lomarev M and Hallett M 2006 Modeling the current distribution during transcranial direct current stimulation *Clin. Neurophysiol.* **117** 1623–9
- Mondino M, Brunelin J, Palm U, Brunoni A R, Fecteau E P and S 2015 Transcranial direct current stimulation for the treatment of refractory symptoms of schizophrenia: current evidence and future directions *Curr. Pharm. Des.* **21** 3373
- Nagaoka T, Watanabe S, Sakurai K, Kunieda E, Watanabe S, Taki M and Yamanaka Y 2004 Development of realistic high-resolution whole-body voxel models of Japanese adult males and females of average height and weight, and application of models to radio-frequency electromagnetic-field dosimetry *Phys. Med. Biol.* **49** 1–15
- Najib U, Bashir S, Edwards D, Rotenberg A and Pascual-Leone A 2011 Transcranial brain stimulation: Clinical applications and future directions *Neurosurg. Clin. North Am.* **22** 233–51

- Nardone R, Versace V, Brigo F, Golaszewski S, Carnicelli L, Saltauari L, Trinka E and Sebastianelli L 2020 Transcranial magnetic stimulation and gait disturbances in Parkinson's disease: a systematic review *Neurophysiol. Clin.* **50** 213–25
- Neuling T, Wagner S, Wolters C H, Zaehle T and Herrmann C S 2012 Finite-element model predicts current density distribution for clinical applications of tDCS and tACS *Front. Psychiatry* **3** 1–10
- Nitsche M A et al 2008 Transcranial direct current stimulation: state of the art 2008 *Brain Stimul.* **1** 203–23
- Nitsche M A and Paulus W 2001 Sustained excitability elevations induced by transcranial DC motor cortex stimulation in humans *Neurology* **57** 1899–901
- Nummenmaa A, Stenroos M, Ilmoniemi R J, Okada Y C, Hamalainen M S and Raji T 2013 Comparison of spherical and realistically shaped boundary element head models for transcranial magnetic stimulation navigation *Clin. Neurophysiol.* **124** 1995–2007
- Okun M S and Zeilman P R 2014 *Parkinson's Disease: Guide to Deep Brain Stimulation Therapy* 2nd edn (National Parkinson Foundation)
- Opitz A, Fox M D, Craddock R C, Colcombe S and Milham M P 2016 An integrated framework for targeting functional networks via transcranial magnetic stimulation *Neuroimage* **127** 86–96
- Opitz A, Windhoff M, Heidemann R M, Turner R and Thielscher A 2011 How the brain tissue shapes the electric field induced by transcranial magnetic stimulation *Neuroimage* **58** 849–59
- Opitz A, Yeagle E, Thielscher A, Schroeder C, Mehta A D and Milham M P 2018 On the importance of precise electrode placement for targeted transcranial electric stimulation *Neuroimage* **181** 560–7
- Opitz A, Zafar N, Bockermann V, Rohde V and Paulus W 2014 Validating computationally predicted TMS stimulation areas using direct electrical stimulation in patients with brain tumors near precentral regions *NeuroImage Clin.* **4** 500–7
- Paffi A, Apollonio F, D'Inzeo G and Liberti M 2013 Stochastic resonance induced by exogenous noise in a model of a neuronal network *Netw. Comput. Neural Syst.* **24** 99–113
- Paffi A, Camera F, Apollonio F, d'Inzeo G and Liberti M 2015a Numerical characterization of intraoperative and chronic electrodes in deep brain stimulation *Front. Comput. Neurosci.* **9** 2
- Paffi A, Camera F, Carducci F, Rubino G, Tampieri P, Liberti M and Apollonio F 2015b A computational model for real-time calculation of electric field due to transcranial magnetic stimulation in clinics *Int. J. Antennas Propag.* **2015** 23–7
- Parazzini M, Fiocchi S, Liorni I and Ravazzani P 2015 Effect of the interindividual variability on computational modeling of transcranial direct current stimulation *Comput. Intell. Neurosci.* **2015** 963293
- Parazzini M, Fiocchi S and Ravazzani P 2012 Electric field and current density distribution in an anatomical head model during transcranial direct current stimulation for tinnitus treatment *Bioelectromagnetics* **33** 476–87
- Parazzini M, Fiocchi S, Rossi E, Paglialonga A and Ravazzani P 2011 Transcranial direct current stimulation: Estimation of the electric field and of the current density in an anatomical human head model *IEEE Trans. Biomed. Eng.* **58** 1773–80
- Parazzini M, Rossi E, Ferrucci R, Liorni I, Priori A and Ravazzani P 2014 Modelling the electric field and the current density generated by cerebellar transcranial DC stimulation in humans *Clin. Neurophysiol.* **125** 577–84
- Priori A, Berardelli A, Rona S, Accornero N and Manfredi M 1998 Polarization of the human motor cortex through the scalp *Neuroreport* **9** 2257–60
- Puonti O, Saturnino G B, Madsen K H and Thielscher A 2019 Comparing and validating automated tools for individualized electric field simulations in the human head bioRxiv:611962 (<https://doi.org/10.1101/611962>)
- Rashed E A, Gomez-Tames J and Hirata A 2019 Human head skin thickness modeling for electromagnetic dosimetry *IEEE Access* **7** 46176–86
- Ray P, Sinha V K and Tikka S K 2015 Adjuvant low-frequency rTMS in treating auditory hallucinations in recent-onset schizophrenia: a randomized controlled study investigating the effect of high-frequency priming stimulation *Ann. Gen. Psychiatry* **14** 8
- Rossini P M et al 2015 Non-invasive electrical and magnetic stimulation of the brain, spinal cord, roots and peripheral nerves: basic principles and procedures for routine clinical and research application: an updated report from an I.F.C.N. Committee *Clin. Neurophysiol.* **126** 1071–107
- Rotenberg A 2010 Prospects for clinical applications of transcranial magnetic stimulation and real-time EEG in epilepsy *Brain Topogr.* **22** 257–66
- Rotenberg A, Horvath J and Pascual-Leone A 2014 *Transcranial Magnetic Stimulation* (New York: Humana Press) (https://doi.org/10.1007/978-1-4939-0879-0_1)
- Ruohonen J and Karhu J 2010 Navigated transcranial magnetic stimulation *Clin. Neurophysiol.* **40** 7–17
- Sadleir R J, Vannorsdall T D, Schretlen D J and Gordon B 2010 Transcranial direct current stimulation (tDCS) in a realistic head model *Neuroimage* **51** 1310–8
- Sadleir R J, Vannorsdall T D, Schretlen D J and Gordon B 2012 Target optimization in transcranial direct current stimulation *Front. Psychiatry* **3** 1–13
- Salinas F S, Lancaster J L and Fox P T 2009 3D modeling of the total electric field induced by transcranial magnetic stimulation using the boundary element method *Phys. Med. Biol.* **54** 3631–47
- Saturnino G B, Thielscher A, Madsen K H, Knösche T R and Weise K 2019 A principled approach to conductivity uncertainty analysis in electric field calculations *Neuroimage* **188** 821–34
- Schmid G, Cecil S and Überbacher R 2013 The role of skin conductivity in a low frequency exposure assessment for peripheral nerve tissue according to the ICNIRP 2010 guidelines *Phys. Med. Biol.* **58** 4703–16
- Schoiswohl S, Agrawal K, Simoes J, Neff P, Schlee W, Langguth B and Schecklmann M 2019 RTMS parameters in tinnitus trials: a systematic review *Sci. Rep.* **9** 1–11
- Sim4Life-v4.4. SIMULATION 4 LIFE Science Platform <http://zurichmedtech.com/sim4life> (Last Accessed: 8th June 2020)
- Soldati M and Laakso I 2020 Computational errors of the induced electric field in voxelized and tetrahedral anatomical head models exposed to spatially uniform and localized magnetic fields *Phys. Med. Biol.* **65** 015001
- Starzyński J, Sawicki B, Wincenciak S, Krawczyk A and Zyss T 2002 Simulation of magnetic stimulation of the brain *IEEE Trans. Magn.* **38** 1237–40
- Tarao H, Kuisti H, Korpinen L, Hayashi N and Isaka K 2012 Effects of tissue conductivity and electrode area on internal electric fields in a numerical human model for ELF contact current exposures *Phys. Med. Biol.* **57** 2981
- Thielscher A, Opitz A and Windhoff M 2011 Impact of the gyral geometry on the electric field induced by transcranial magnetic stimulation *Neuroimage* **54** 234–43
- Truong D Q, Magerowski G, Blackburn G L, Bikson M and Alonso-Alonso M 2013 Computational modeling of transcranial direct current stimulation (tDCS) in obesity: Impact of head fat and dose guidelines *NeuroImage Clin.* **2** 759–66
- Tsai B, Xue H, Birgersson E, Ollmar S and Birgersson U 2019 Dielectrical properties of living epidermis and dermis in the frequency range from 1 kHz to 1 MHz *J. Electr. Bioimpedance* **10** 14–23

- Valero-Cabré A, Pascual-Leone A and Coubard O A 2011 Transcranial magnetic stimulation (TMS) in basic and clinical neuroscience research *Rev. Neurol.* **167** 291–316
- Vanhaerents S, Chang B S, Rotenberg A, Pascual-Leone A and Shafi M M 2020 Noninvasive brain stimulation in epilepsy *J. Clin. Neurophysiol.* **37** 118–30
- Wagner S, Rampersad S M, Aydin Ü, Vorwerk J, Oostendorp T F, Neuling T, Herrmann C S, Stegeman D F and Wolters C H 2014 Investigation of tDCS volume conduction effects in a highly realistic head model *J. Neural Eng.* **11** 016002
- Wagner T A, Zahn M, Grodzinsky A J and Pascual-Leone A 2004 Three-dimensional head model simulation of transcranial magnetic stimulation *IEEE Trans. Biomed. Eng.* **51** 1586–98
- Watanabe K, Kudo Y, Sugawara E, Nakamizo T, Amari K, Takahashi K, Tanaka O, Endo M, Hayakawa Y and Johkura K 2018 Comparative study of ipsilesional and contralesional repetitive transcranial magnetic stimulations for acute infarction *J. Neurol. Sci.* **384** 10–4
- Weber M and Eisen A A 2002 Magnetic stimulation of the central and peripheral nervous systems *Muscle and Nerve* **25** 160–75
- Weise K, Numssen O, Thielscher A, Hartwigsen G and Knösche T R 2020 A novel approach to localize cortical TMS effects *Neuroimage* **209** 116486
- Windhoff M, Opitz A and Thielscher A 2013 Electric field calculations in brain stimulation based on finite elements: An optimized processing pipeline for the generation and usage of accurate individual head models *Hum. Brain Mapp.* **34** 923–35
- Xu H and Mandal M 2015 Epidermis segmentation in skin histopathological images based on thickness measurement and k-means algorithm *Eurasip J. Image Video Process.* **2015** 1–14
- Yamamoto T and Yamamoto Y 1976 Electrical properties of the epidermal stratum corneum *Med. Biol. Eng.* **14** 151–8
- Yang S and Chang M C 2020 Effect of repetitive transcranial magnetic stimulation on pain management: a systematic narrative review *Front. Neurol.* **11** 114
- Zhao N, Zhang J, Qiu M, Wang C, Xiang Y, Wang H, Xie J, Liu S and Wu J 2018 Scalp acupuncture plus low-frequency rTMS promotes repair of brain white matter tracts in stroke patients: a DTI study *J. Integr. Neurosci.* **17** 125–39
- Zhou D-D, Wang W, Wang G-M, Li D-Q and Kuang L 2017 An updated meta-analysis: short-term therapeutic effects of repeated transcranial magnetic stimulation in treating obsessive-compulsive disorder *J. Affect. Disord.* **215** 187–96